MEMS spatial light modulators for controlled optical transmission through nearly opaque materials

Thomas Bifano*[a], Yang Lu[a], Christopher Stockbridge[a], Aaron Berliner[a], John Moore[a], Richard Paxman[b], Santosh Tripanthi[c], Kimani Tousssaint[d]
[a]Boston University Photonics Center, 8 Saint Mary's St., Boston, MA 02215;
[b]Paxman Consulting, 9228 Sunset Lake Dr., Saline, MI 48176
[c]Electrical and Computer Engineering, University of Illinois at Urbana-Champaign, 1206 W. Green St., Urbana, IL 61801
[d]Mechanical Science and Engineering, University of Illinois at Urbana-Champaign, 1206 W. Green St., Urbana, IL 61801

ABSTRACT

A reflective microelectromechanical mirror array was used to control the intensity distribution of a coherent beam that was propagated through a strongly scattering medium. The controller modulated phase spatially in a plane upstream of the scattering medium and monitored intensity spatially in a plane downstream of the medium. Optimization techniques were used to maximize the intensity at a single point in the downstream plane. Intensity enhancement by factors of several hundred were achieved within a few thousand iterations using a MEMS segmented deformable mirror (e.g. a spatial light modulator) with 1020 independent segments. Experimental results are reported for alternate optimization approaches and for optimization through dynamically translating scattering media.

Keywords: Adaptive optics, deformable mirror, scattering

1. INTRODUCTION

In recent years, a number of research groups have reported on controlled propagation through scattering media [*1-6*]. Using liquid-crystal spatial light modulators (LC-SLMs) to pre-compensate the wavefront of a coherent beam, these groups have demonstrated the capacity to generate diffraction-limited far-field intensity control through feedback-based optimization. They have also empirically characterized optical transmission matrices for systems that include static scattering media. Such transmission matrices might ultimately permit direct imaging through what would otherwise be considered a nearly opaque material.

A limitation of this new approach to shaping light through disordered media is that it requires some form of blind optimization, and the time required for convergence of the optimization scales with the number independent segments in the SLM, and with its frame refresh rate. To date, that convergence time is measured in minutes or hours. The work presented here describes experimental results on optical transmission through nearly opaque media and focusing using a microelectromechanical system (MEMS) SLM [*7*], which can reduce optimization times by up to three orders of magnitude.

2. EXPERIMENTAL SETUP

A schematic representation and a photograph of the experimental setup are depicted in Figure 1.

The MEMS SLM (Boston Micromachines Corporation kiloDM) is comprised of 1020 controllable mirror segments in a 32 by 32 array (with immobile mirror segments at the four corners of the array). Each segment measures 300μm square and 3μm thick and can be translated in a surface-normal direction using voltage control to an underlying electrostatic actuator. Each segment translation is controllable with ~0.01 nanometer precision over a range of ~1.5μm. The SLM was pre-calibrated using a surface mapping interferometer (Zygo NewView 6300), to allow subsequent direct phase control with ~0.01 wave accuracy at the laser wavelength of 532nm. The SLM can be updated at a frame rate of

MEMS Adaptive Optics VI, edited by Scot S. Olivier, Thomas G. Bifano, Joel Kubby, Proc. of SPIE Vol. 8253, 82530L · © 2012 SPIE · CCC code: 0277-786X/12/$18 · doi: 10.1117/12.911384

~30kHz. The camera used for feedback control and optimization was a CMOS device (IDS Imaging uEye) capable of a frame rate of 350Hz for the 32 by 32 pixel subarray used in these experiments.

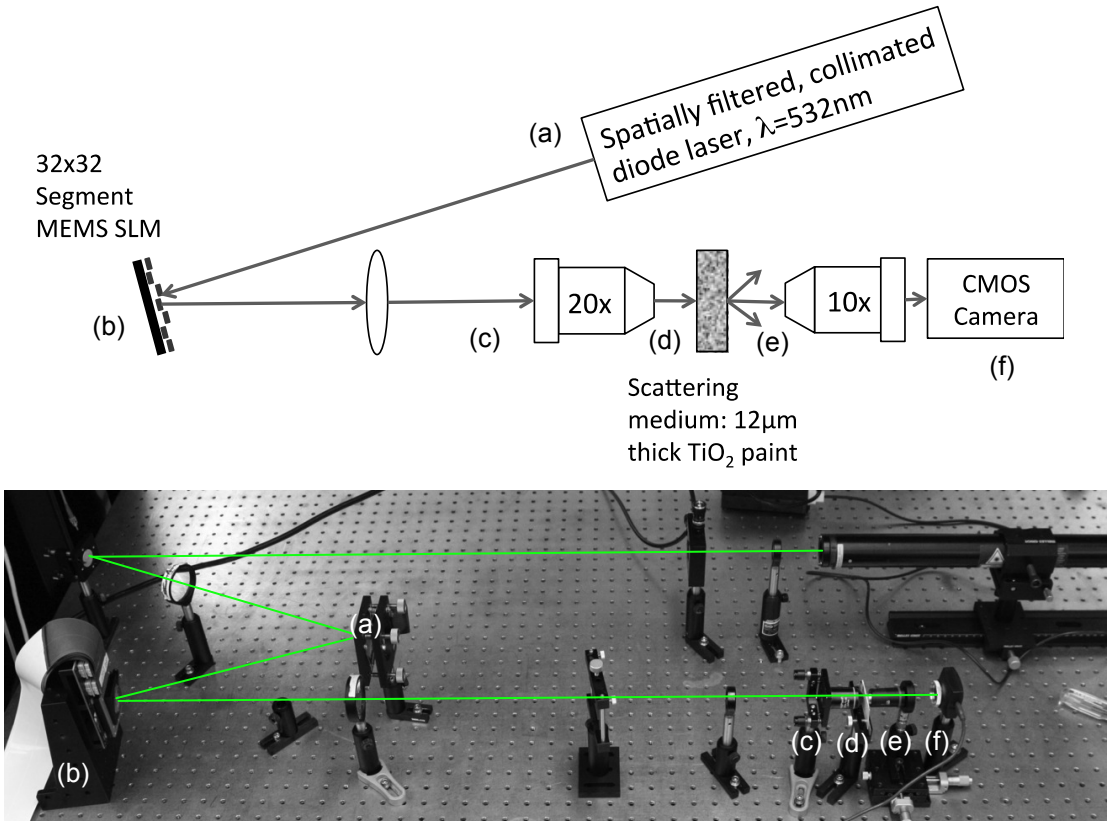

Figure 1. Schematic of the experimental apparatus. A collimated, spatially filtered laser beam, (a), reflects from the SLM surface, (b), acquiring a spatially distributed phase shift. The wavefront at the SLM is reimaged at 45× by a 45× telescope comprised of a 400mm focal length lens and a 20×, 0.4NA microscope objective, (c) onto the front surface of the scattering medium, (d). The scattering medium is a 12μm thick film of white paint deposited on a glass slide. A 10x microscope objective on the far side of the scattering medium, (e), projects a portion of the resulting speckle pattern onto a fixed detector, (f).

Prior to optimization, the nearly opaque medium caused the optical intensity at the camera to be high-contrast, fully developed speckle. The optimization objective was to collect as much intensity as possible into a single speckle at the center of the camera subarray. The 10x objective was translated along the optical axis so that the mean diameter (measured as its full-width-half-maximum amplitude) of a single speckle was roughly 10μm, twice the size of the camera pixel.

One algorithm used for optimization was stochastic parallel gradient descent (SPGD), which has been used with some success in adaptive optics applications previously [*8-11*]. A second algorithm tested was Walsh function optimization, which has also been used previously in adaptive optics applications [*12, 13*].

For SPGD optimization, the SLM is initially flattened by providing a known array of inputs U^{xy} to its actuator array, and for each optimization iteration (n), every mirror segment is perturbed simultaneously by a fixed, small phase step Δu. The *direction* of the phase shift for each mirror segment is randomly assigned at each iteration for each actuator (R^{xy}=+/-*1*). A scalar measure (J^{+}) of the desired optimization objective is made (in this case, measured intensity at the camera center) after the perturbation. The perturbation is then applied in the *opposite direction* for all segments, and a second measure (J^{-}) of the desired objective is made. The inputs to the entire array of mirror segments are then updated using parallel integral feedback based on the partial derivative of the objective function:

$$U_n^{xy} = U_{n-1}^{xy} + kR_n^{xy}(\Delta u)(J_n^+ - J_n^-), \quad (1)$$

where k is a control gain factor. The optimal perturbation step size was determined to be 0.03 waves in a series of statistical optimization experiments. Note that SPGD optimization used here to compensate for scattering (turbid) media is closely related to the stochastic method originally proposed by Muller and Buffington [*14*] for correcting wavefronts aberrated by turbulent media (the atmosphere).

For Walsh optimization the mirror is perturbed in a sequence of 1024 orthonormal binary patterns corresponding to Walsh matrices [*15*]. Each square Walsh matrix W^{xy} (32 by 32 in the present case) has the characteristic its entries are +1 or −1, and the property that the dot product of any two distinct rows (or columns) is zero. A collection of 1024 Walsh matrices represents a complete and compact basis set for the SLM: all possible states can be produced using a linear combination of scaled Walsh matrix inputs if each actuator in the SLM is made to correspond with a corresponding entry in the Walsh matrix. To implement Walsh optimization, the SLM is initially flattened by providing a known array of inputs U^{xy} to its actuators, and a scalar measure (J^0) of the desired optimization objective is made. For each of Walsh matrix $W^{xy}{}_n$, every SLM actuator that has an associated Walsh matrix value of +1 is perturbed by a fixed, phase step Δu (typically, but not necessarily, λ/4) while segments that have an associated Walsh matrix value of -1 are left unperturbed. Then a scalar measure (J^+) of the desired optimization objective is made. Next, the phase step is reversed in direction ($-\Delta u$) and another scalar measure (J^-) of the desired optimization objective is made. Finally, the optimal scalar value of phase shift is calculated using a standard technique for three-point phase shifting interferometry [*16*], and the SLM is updated as follows:

$$U_n^{xy} = U_{n-1}^{xy} + \left(\frac{W_n^{xy}+1}{4\pi}\right)\tan^{-1}\left(\frac{(J_n^- - J_n^+)\tan\left(\frac{\pi}{\Delta u}\right)}{-J_n^- + 2J_n^0 - J_n^+}\right) - \frac{1}{4} \quad (2)$$

A measure of the optimization objective made after the SLM is updated becomes $J^0{}_{n+1,}$ and the process is repeated for all 1024 Walsh matrices.

Optimization rate was found to be approximately the same for both SPGD and Walsh optimization. Walsh optimization was ultimately preferred, because it is less dependent on control parameters than SPGD optimization.

3. RESULTS

Typical SPGD optimization results are depicted in Figure 2. Optimization reaches an enhancement level (defined as the optimized final peak intensity divided by the spatial mean of the initial image intensity) of ~150 in 3000 iterations with both the SPGD and the Walsh optimization algorithms. The convergence plot is illustrated in Figure 3.

To study the characteristics of an optimized state and its sensitivity to the precise propagation path through the scattering medium, an experiment was conducted in which optimization was first performed with a goal of maximizing intensity on the camera's central pixel. After optimization, the final SLM state was retained as the new *initial* state for the SLM, and optimization was repeated with a revised objective to maximize the intensity of an *adjacent* camera pixel, 5μm from the camera center. Since the speckle size at the camera was two pixels wide, it was not surprising that in an initially optimized state, the adjacent pixel was already at nearly half its optimal intensity. Re-optimization proceeded more rapidly as a result. However, re-optimization with an objective to maximize the intensity at a location two pixels (10μm) away from the center was found to gain no advantage or disadvantage starting from the initially optimized state (Figure 4).

The sensitive dependence of optimization state on precise beam geometry through the medium implies that optimization in the presence of relative motion might be challenging. To explore those challenges, an experiment was devised in which the scattering medium was translated using a precise piezoelectric inchworm translator (Burleigh) after successful optimization. Translation by 1μm without continued optimization reduced the previously optimized

peak intensity by half, and translation by 2μm reduced it to background levels. However, with continued optimization (in this case, SPGD control) the system could maintain optimized intensity at the camera's central location for translational speeds of up to 20nm/sec. At translation speeds between 20nm/sec and 100nm/sec, continued feedback control was effective for some time, but eventually failed, resulting in decay of optimized intensity to background levels. At translation speeds above 100nm/sec, continued feedback had negligible effect. Results are summarized in the plot in Figure 5.

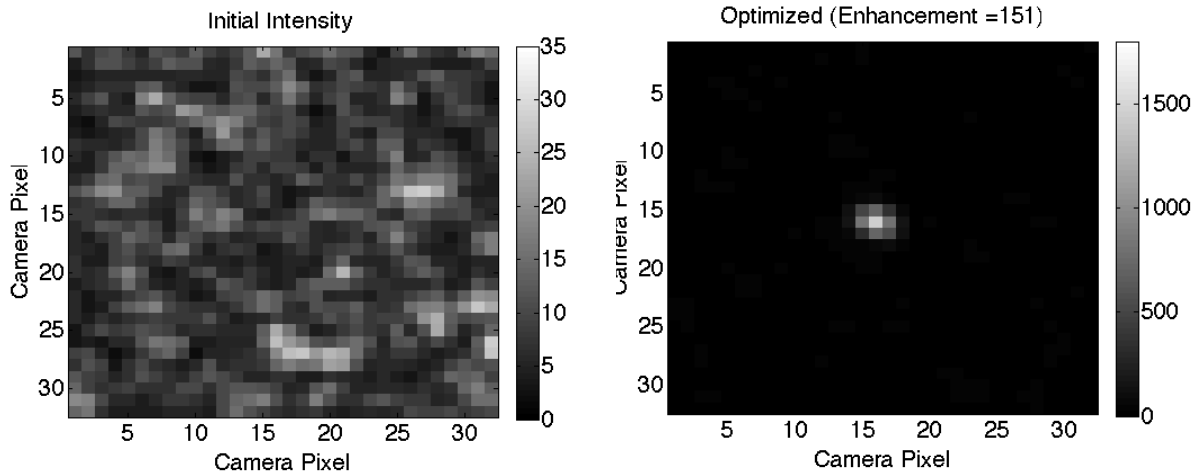

Figure 2. Typical optimization results. Left: Initial speckle pattern measured at the camera plane over an area of 32 by 32 pixels. Speckle size is approximately two pixels in diameter. Right: Final intensity distribution after optimization. Since the camera dynamic range is only eight bits, a variable neutral density filter wheel was adjusted periodically over the course of the experiment. Intensity values are corrected for neutral density setting. At the conclusion of optimization, the peak intensity of the central pixel in the image shown reached a value 151 times larger than the spatial mean of the initial image intensity.

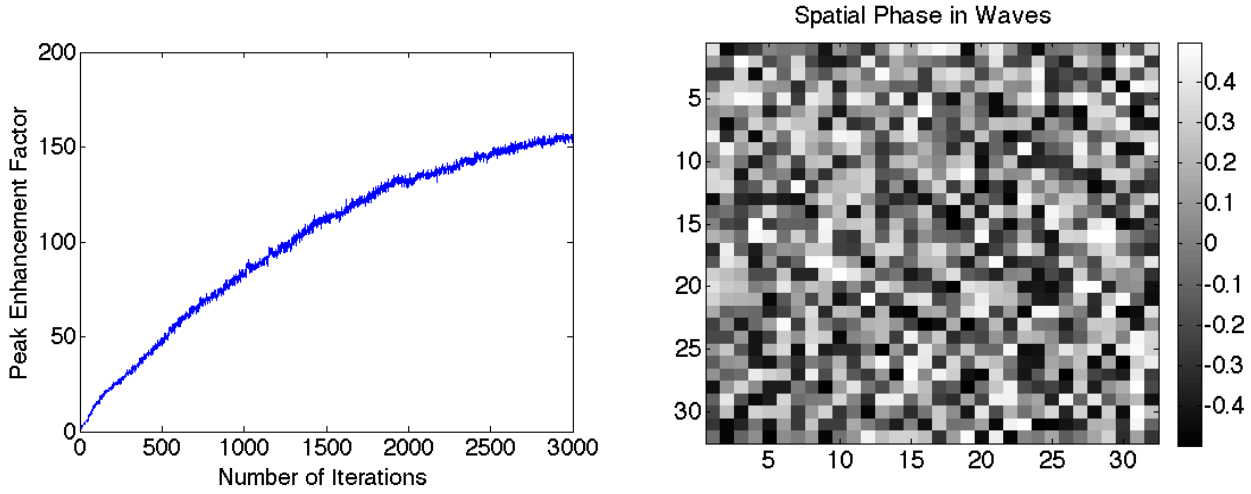

Figure 3. Left: A plot of the normalized, measured peak intensity (i.e. enhancement factor) at the central pixel of the camera as a function of iteration number. Right: Final SLM phase map in waves. Statistical analysis of a number of optimizations confirmed that 1) Adjacent mirror segment phases for optimization were uncorrelated (e.g., randomly distributed) and 2) Successive optimizations with unchanged initial conditions produced final SLM phase states that were uncorrelated with one another.

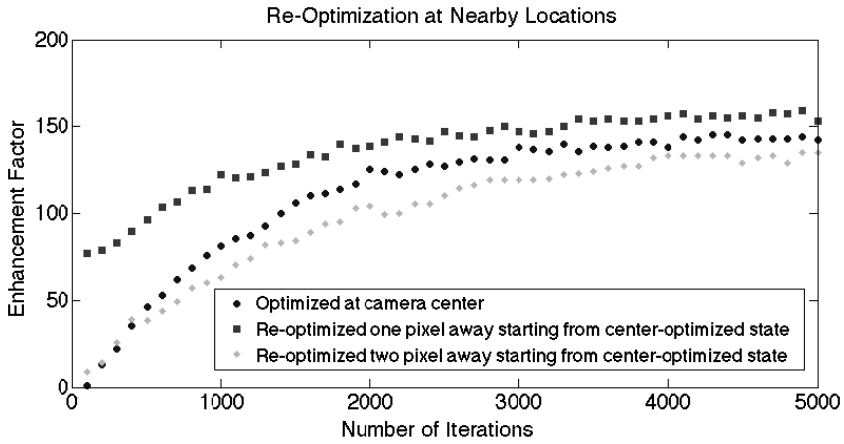

Figure 4. Plots detailing results of optimizing at the central pixel, and then using that optimized state as a starting condition for re-optimization with a goal of maximizing intensity at a nearby location. While some advantage was found in using this starting state to optimize an adjacent pixel, no advantage was retained in optimization for the next pixel (two away from the original location). This suggests that the optimization is sensitive at the micrometer-scale to the precise path taken through the scattering medium.

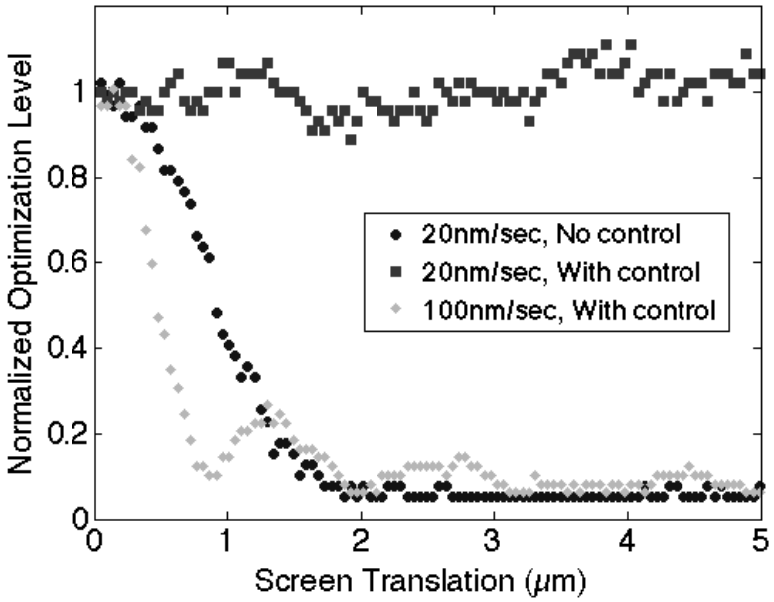

Figure 5. Translation experiment results. After optimizing intensity at the camera center with a fixed scattering medium, the medium was translated both with and without continued control. Without control, optimization was reduced to background levels after 2μm of translation. With control, the optimization was maintained for translational speeds up to 20nm/sec.

One adaptive optics compensation strategy has been shown to be effective in propagating beams through a frozen but translating thin medium of turbulence (phase screen) – a scenario similar to the translation experiments described above. If an estimate can be made of the lateral shift of the medium with respect to the optical axis, a spatially shifted version of the previously optimized SLM state can be used as an initial state for re-optimization. Since it is not practical

to translate the SLM itself, one can instead shift the *pattern* on the SLM by a fixed amount corresponding to the known translation of the medium (and accounting for optical system magnification). This technique begins with an optimized state, and then shifts the pattern on the optimized SLM array by an amount proportional to the expected medium translation. It can then be expected that a substantial amount of the previous optimization would be preserved in the shifted state. Moreover, it would be expected that re-optimization in the shifted state would be faster and more efficient.

In a proof-of-principle experiment, after initial optimization the SLM pattern was shifted by exactly one column (e.g. a 300μm pattern shift), which would correspond optically to a 6.7μm translation of the scattering medium due to the 45× telescope between the two. The peak central intensity on the camera was monitored as a function of medium translation. It was found that the optimization peak reached about half of its original value at the expected translation. Note that the peak location was no longer at the camera center. Re-optimization targeted enhancing the peak at its new location, not the camera center. In this case, re-optimizing was much faster than the initial optimization. Results are illustrated in Figure 6.

In a final experiment, the system was optimized for each of the 32 by 32 camera pixels, and the final SLM optimized state was stored for each camera pixel location. A one-bit pattern replicating the BU logo was prepared, and the SLM was commanded to time-multiplex between the states associated with each pixel in the map having a binary value of 1. That is, the SLM was commanded to dwell at states that would illuminate each of the requested pixels in the camera image for about 100μs, rastering through them in a continuous, 11ms loop. The camera, configured to operate in open loop at a frame rate of 30Hz (e.g., 33ms refresh), averaged the resulting illumination to provide a smooth image as shown in Figure 7.

4. CONCLUSIONS

In this paper, we have reported the use of a MEMS SLM to focus coherent light by pre-compensating prior to encountering nearly opaque scattering media. Whereas the experiments reported are limited by camera speed, with the aid of a high-speed camera, the MEMS device will accommodate increased optimization speeds by up to 3 orders of magnitude relative to the current state-of-the-art. Experiments indicate that the compensation changes rapidly with scan position in the camera array for static scattering media. Therefore, an adaptive system that maintains compensation with dynamic scattering media in the form of translation needs to update rapidly. This capability was demonstrated for scattering media translating at 20nm/sec. An experiment was performed to quantify the value of shifting the pattern on the MEMS SLM on concert with the translating scattering medium. The results suggest the use of a feed-forward strategy in certain scenarios. Finally, an image was transmitted through nearly opaque media through the use of scanning with pre-determined compensation for each raster location.

Increased temporal bandwidth is needed to accommodate scattering media with increased dynamics, including greater rates of bulk translation and eventually scatterers that evolve on a microscopic scale such as fog, smoke, or human tissue. In future work we plan to increase the temporal bandwidth of our adaptive system by using high-speed cameras and improved optimization algorithms.

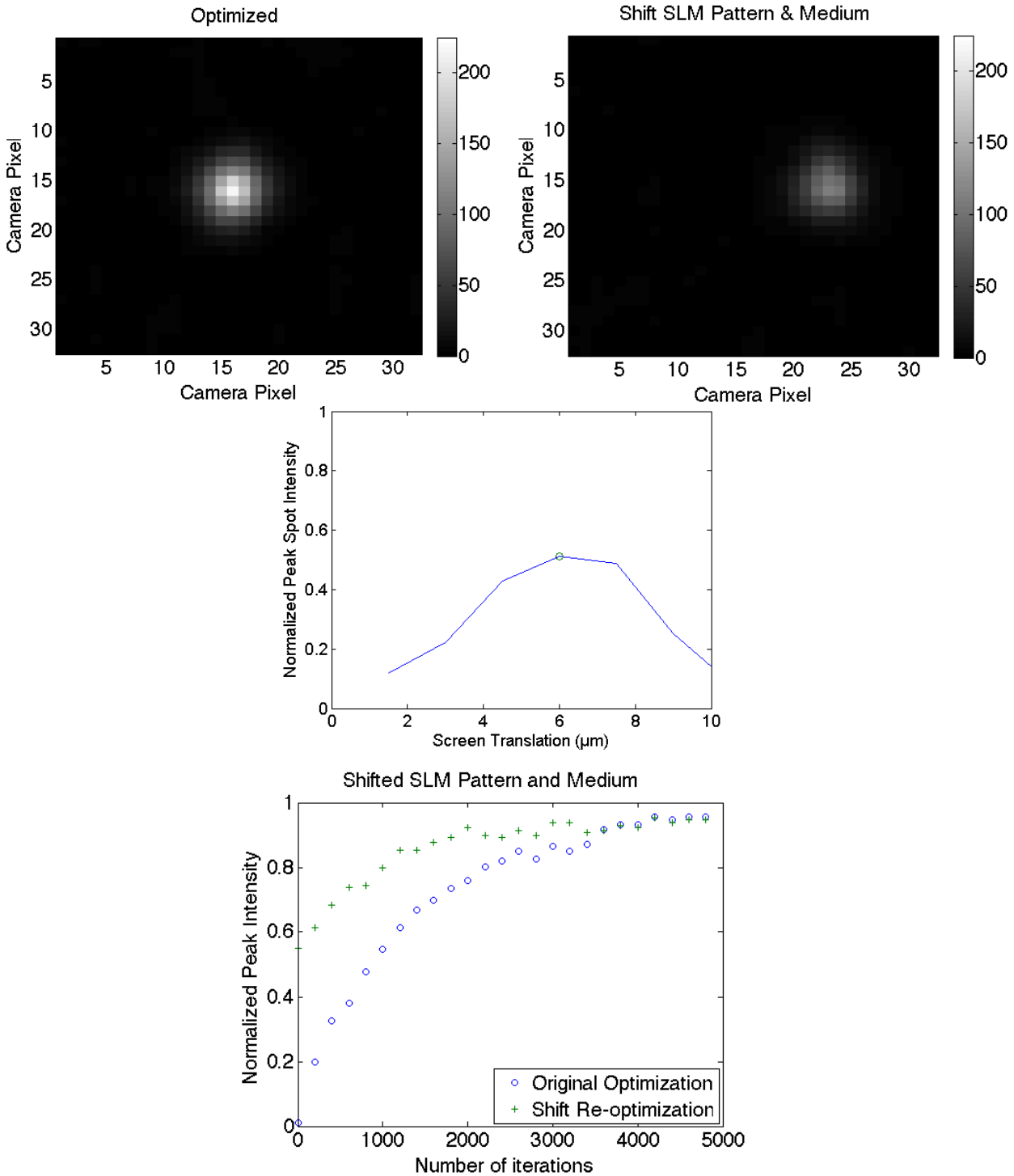

Figure 6. "Frozen screen" translation experiment results. Top left: Initial optimized focus at camera center. Top right: Observed focus after coordinated shift of SLM and scattering medium. Middle: Plot of peak observed intensity on the camera as a function of medium translation. The circled data point corresponds to the upper right figure. Bottom: Plots of initial optimization and re-optimization after dual translation.

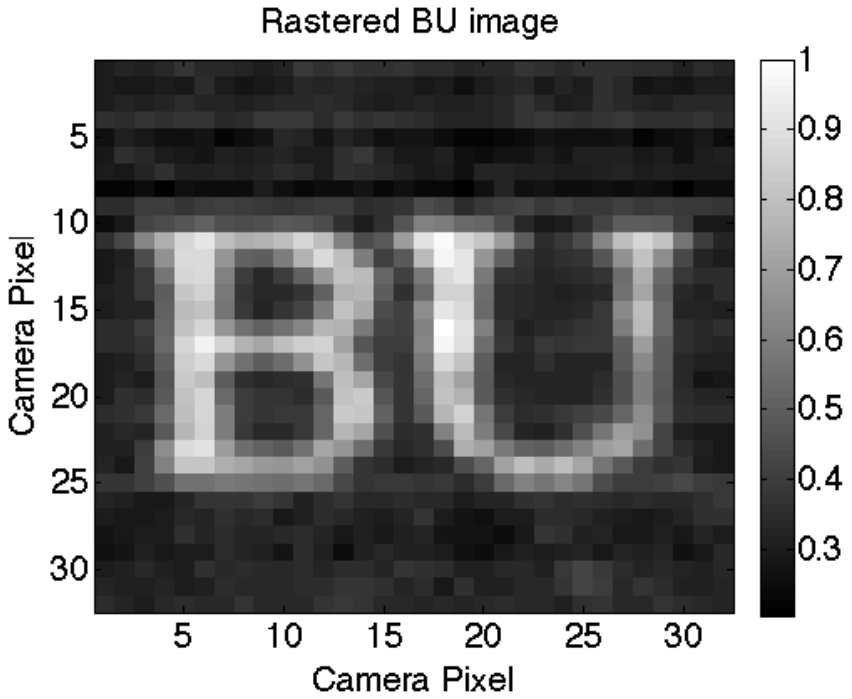

Figure 7. Camera image of projected, rastered illumination of a prescribed pattern through a highly scattering medium at normal video rate.

REFERENCES

[1] Popoff SM, Lerosey G, Carminati R, Fink M, Boccara AC, Gigan S, "Measuring the Transmission Matrix in Optics: An Approach to the Study and Control of Light Propagation in Disordered Media," *Physical Review Letters*, [104], 100601, (2010).

[2] Popoff SM, Lerosey G, Fink M, Boccara AC, Gigan S, "Image Transmission Through an Opaque Material," *Nature Communications*, [1], (2010).

[3] Lerosey G, de Rosny J, Tourin A, Fink M, "Focusing Beyond the Diffraction Limit with Far-Field Time Reversal," *Science*, [315], 1120-1122, (2007).

[4] vanPutten EG, Mosk AP, "The information age in optics: Measuring the transmission matrix," *Physics*, [3], 22, (2010).

[5] Vellekoop IM, Mosk AP, "Focusing coherent light through opaque strongly scattering media," *Opt. Lett.*, [32], 2309-2311, (2007).

[6] Vellekoop IM, LagendijkA, Mosk AP, "Exploiting disorder for perfect focusing," *Nat Photon*, [4], 320 - 322, (2010).

[7] Bifano T, "Adaptive imaging: MEMS deformable mirrors," *Nat Photon*, [5], 21-23, (2011).

[8] Vorontsov M, Riker J, Carhart G, Rao Gudimetla VS, Beresnev L, Weyrauch T, Roberts JLC, "Deep turbulence effects compensation experiments with a cascaded adaptive optics system using a 3.63 m telescope," *Appl. Opt.*, [48], A47-A57, (2009).

[9] Weyrauch T, Vorontsov MA, Bifano TG, Hammer JA, Cohen M, Cauwenberghs G, "Microscale adaptive optics: wave-front control with a mu-mirror array and a VLSI stochastic gradient descent controller," *Applied Optics*, [40], 4243-4253, (2001).

[10] Vorontsov MA, Sivokon VP, "Stochastic parallel-gradient-descent technique for high-resolution wave-front phase-distortion correction," *J. Opt. Soc. Am. A*, [15], 2745-2758, (1998).

[11] Vorontsov MA, Carhart GW, Ricklin JC, "Adaptive phase-distortion correction based on parallel gradient-descent optimization," *Opt. Lett.*, [22], 907-909, (1997).

[12] Wang F, "Control of deformable mirror with light-intensity measurements through single-mode fiber," *Appl. Opt.*, [49], G60-G66, (2010).
[13] Wang F, "Wavefront sensing through measurements of binary aberration modes," *Appl. Opt.*, [48], 2865-2870, (2009).
[14] Muller RA, Buffington A, "Real-time correction of atmospherically degraded telescope images through image sharpening," *J. Opt. Soc. Am.*, [64], 1200-1210, (1974).
[15] Walsh JL, "A Closed Set of Normal Orthogonal Functions," *American Journal of Mathematics*, [45], 5-24, (1923).
[16] Schreiber H, Bruning JH, in *Optical Shop Testing*. (John Wiley & Sons, Inc., 2006), pp. 547-666, 2006.